Cluster Ions: Carbon, Met-cars, and σ-Bond Activation

MICHAEL T. BOWERS

Department of Chemistry, University of California, Santa Barbara, California 93106

Received July 20, 1994

I. Introduction

The subject matter for this Account, "cluster ions", has become a huge and rapidly expanding field during the past decade, and consequently, any rendition requires judicious selection by the author. However, by explicit editorial exclusion, Accounts are not reviews, and consequently, one should look elsewhere for one of the many excellent reviews or compendiums on the subject.[1-10] An Account is, by editorial edict, about "a topic of intense interest to the author and to a considerable extent treats the author's own experimental or theoretical results." This spirit will guide this paper, hopefully in a way where general principles are extracted from the results and details left to publication in more appropriate journals. I do want to make one general point, however. Information obtained from ionic clusters can often be used to infer properties of the corresponding neutrals. In metal clusters, for example, neutral and ionic reactivities can become very similar at sizes as small as five of six atoms.[10] In addition, C_{60}, buckminsterfullerene, was detected and correctly identified using mass spectrometry[11] many years before it was synthesized in the bulk.[12] Both of these examples, and all of those discussed in this Account, take advantage of the fact that charged clusters can employ the powerful tools of modern mass spectrometry so nicely exemplified throughout this special issue.

In this Account we will discuss several aspects of clusters of substantial current interest to us. Topics will include growth processes in metal/carbon composites, including met-cars[13] (metallocarbohedranes) and other interesting structures;[14] we will address the question of why there appear to be no polycyclic aromatic hydrocarbon (PAH) type "building" blocks along the way to fullerene formation in pure carbon clusters;[15-17] and finally, the question of σ-bond activation of small molecules by transition metal centers will be addressed, with a focus on how and why these important processes are cluster assisted.

II. Experimental Conditions

A detailed description of the apparatus used in the work outlined here has been published previously,[15,18-20] and only a functional description will be given. A more thorough discussion will be given of the mobility/ion chromatography aspects of our experiment since these are unique to the kind of work we do. A number of different ion sources are available. These include a traditional electron ionization (EI) source, a surface ionization (SI) source, and a Smalley type[21] laser desorption–supersonic expansion (LD–SSE) source. In this paper, the LD–SSE source is used for the carbon-based clusters and the metallo/carbon clusters and either the EI or SI source is used for the remainder of the work. All sources float at 5 kV and are coupled to a reverse geometry magnetic sector/electric sector double-focusing machine used for initial mass analysis. A mass-selected beam is then decelerated to 1 or 2 eV and focused on the small entrance hole of a high-pressure drift cell. Ions drift through the cell under the influence of a small, variable uniform electric field in the presence of either

Michael Bowers grew up in Spokane, WA, and attended Gonzaga University, receiving a B.S. in chemistry in 1962 and being named outstanding senior student. His graduate work was done at the University of Illinois as an NSF Fellow, where he received his Ph.D. under the guidance of Prof. Bill Flygare in 1966. After two years in the Army, at the Jet Propulsion Laboratory, in 1968 he became an assistant professor at University of California at Santa Barbara, where he is currently a professor of chemistry. Bowers is a Fellow of the American Physical Society, was awarded the Nobel laureate Signature Award (ACS) with his student Nicholas Kirchner, was selected as the Faculty Research Lecturer at UCSB for 1994, and is currently a Guggenheim Fellow.

(1) See, for example, the following journal issues devoted soley to clusters: *Acc. Chem. Res.* **1992**, *25*, No. 3; *Int. J. Mass Spectrom. Ion Processes* **1990**, *102*; *J. Phys. Chem.* **1987**, *91*, No. 10; *Chem. Rev.* **1986**, *86*, No. 3; *Z. Phys. D* **1986**, *3*, No. 2/3; **1991**, *19*, *20*; **1993**, *26*; *Surf. Sci.* **1985**, *156*.

(2) Castleman, A. W.; Keesee, R. G. *Annu. Rev. Phys. Chem.* **1986**, *37*, 325.

(3) Weltner, W.; van Zee, R. *Chem. Rev.* **1989**, *89*, 1713.

(4) Scoles, G., Ed. *The Chemical Physics of Atomic and Molecular Clusters*; North-Holland: Amsterdam, 1990.

(5) Bernstein, E. R., Ed. *Atomic and Molecular Clusters*; Elsevier: New York, 1990.

(6) Parent, D. C.; Anderson, S. L. *Chem. Rev.* **1992**, *92*, 1541.

(7) Märk, T. D.; Castleman, A. W. *Adv. At. Mol. Phys.* **1984**, *20*, 65.

(8) Maier, J. P., Ed. *Ion and Cluster Ion Spectroscopy and Structure*; Elsevier: Amsterdam, 1989.

(9) Benedek, G.; Martin, T. P., Pacchioni, G., Ed. *Elemental and Molecular Structures*; Springer: Berlin, 1988.

(10) Zakin, M. R.; Brinkman, R. D.; Cox, D. M.; Kaldor, A. *J. Chem. Phys.* **1988**, *88*, 3555.

(11) Kroto, H. W.; Heath, J. R.; O'Brien, S. C.; Curl, R. F.; Smalley, R. E. *Nature* **1985**, *318*, 162. Zhang, Q. L., O'Brien, S. C.; Heath, J. R.; Lui, Y.; Curl, R. F.; Kroto, H. W.; Smalley, R. E. *J. Phys. Chem.* **1986**, *90*, 525.

(12) Krätschmer, W.; Fostiropoulos, K.; Huffman, D. R. *Chem. Phys. Lett.* **1990**, *170*, 167. Meijer, G.; Bethune, D. S. *Chem. Phys. Lett.* **1990**, *125*, 1. Haufler, R. E.; Conceicao, J.; Chibante, L. P. F.; Chai, Y.; Byrne, N. E.; Flanagan, S.; Haley, M. M.; O'Brien, S. C.; Pan, C.; Xiao, Z.; Billups, W. E.; Ciufolini, M. A.; Hauge, R. H.; Margrave, J. L.; Wilson, L. J.; Curle, R. F.; Smalley, R. E. *J. Phys. Chem.* **1990**, *94*, 8634. Taylor, R.; Hane, J. P.; Abdulsada, A. K.; Kroto, H. W. *J. Chem. Soc., Chem. Commun.* **1990**, N20, 1423.

(13) For early references, see: Guo, B. C.; Kerns, K. P.; Castleman, A. W. *Science* **1992**, *255*, 1411. Wei, S.; Guo, B. C.; Pernell, J.; Buzza, S.; Castleman, A. W. *J. Phys. Chem.* **1992**, *96*, 4166. Guo, B. C.; Wie, S.; Pernell, J.; Buzza, S.; Castleman, A. W. *Science* **1992**, *256*, 515.

(14) (a) Pilgrim, J. S.; Duncan, M. A. *J. Am. Chem. Soc.* **1993**, *115*, 4395; (b) 6985, (c) 9724; (d) *Int. J. Mass Spectrom Ion Processes*, in press.

(15) (a) von Helden, G.; Hsu, M.-T.; Kemper, P. R.; Bowers, M. T. *J. Chem. Phys.* **1991**, *95*, 3835. (b) von Helden, G.; Hsu, M.-T.; Gotts, N.; Bowers, M. T. *J. Phys. Chem.* **1993**, *97*, 8182.

(16) von Helden, G.; Gotts, N.; Bowers, M. T. *Nature* **1993**, *363*, 60; *J. Am. Chem. Soc.* **1993**, *115*, 4363.

(17) Hunter, J.; Fye, J.; Jarrold, M. F. *Science* **1993**, *260*, 784.

(18) Kemper, P. R.; Bowers, M. T. *J. Am. Soc. Mass Spectrom.* **1990**, *1*, 197.

(19) Bowers, M. T.; Kemper, P. R.; von Helden, G.; van Koppen, P. A. M. *Science* **1993**, *260*, 1446.

(20) von Helden, G.; Hsu, M.-T.; Gotts, N.; Bowers, M. T. *J. Phys. Chem.* **1993**, *97*, 8182.

(21) Powers, D. E.; Hansen, S. G.; Geusic, M. E.; Puiu, A. C.; Hopkins, J. B.; Dietz, T. G.; Duncan, M. A.; Langridge-Smith, P. R. R.; Smalley, R. E. *J. Phys. Chem.* **1982**, *86*, 2556.

0001-4842/94/0127-0324$04.50/0

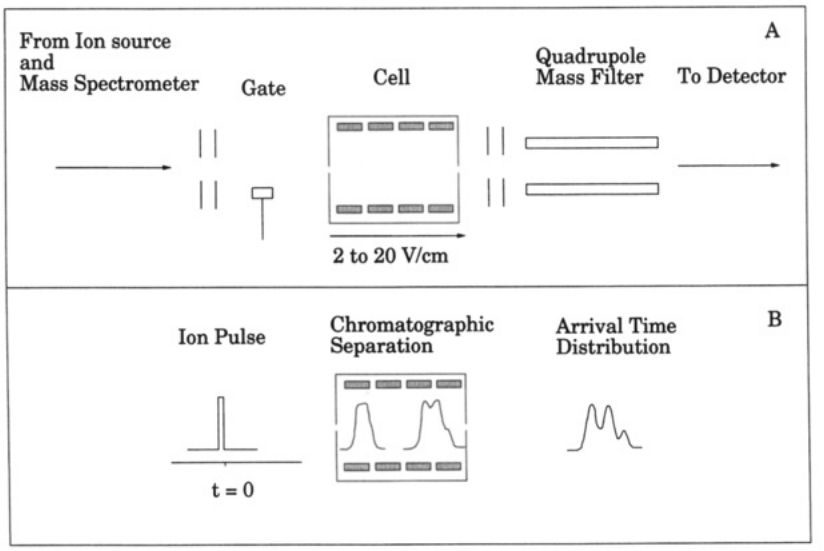

Figure 1. Schematic of the ion chromatography experiment. (A) A beam of mass-selected ions is focused on the 0.5-mm entrance hole of the IC cell which contains 2−5 Torr of He gas for an IC experiment. For a clustering experiment the reagent gas (H_2 or CH_4) is substituted for He. In the IC experiment a 1−10-μs pulse of ions is injected at low energy (2−3 eV lab). For the clustering studies a continuous beam is injected. The ions drift through the cell under the influence of a weak electric field. The ions exit the cell and are mass selected, analyzed, and detected. (B) This panel schematically shows how ions with different collision cross sections with He are spatially and temporally separated in the IC cell.

He buffer gas, clustering reagent gas, or a mixture of the two. They emerge through another small hole and are mildly accelerated, pass through a quadrupole mass filter, and are detected.

Two different kinds of experiments will be described. In the first set, the drift cell will be used in its ion chromatography (IC) mode. In this instance a gate located prior to the cell is pulsed to let in a narrow burst of mass-selected ions (1−5 μs). The ion cloud will undergo 10^5−10^6 collisions with a He buffer gas while transiting the cell. If the beam is composed of several species with different collision cross sections with He, those with the larger cross sections will be spatially and temporally separated from those with smaller cross sections. If time is set to 0 when the gate is opened, then an arrival time distribution (ATD) will be observed at the detector at some later time. This ATD will be composed of a separate peak for each species present, with the area under each peak directly related to the fractional abundance of the species present. This entire process is schematically shown in Figure 1.

For heavy ions colliding with light neutral particles,[22] the following important equations are readily derived:[19,23]

$$t_d(1) = \frac{\sigma(1)}{\sigma(2)} t_d(2) \tag{1a}$$

$$t_d(1) - t_d(2) = \frac{z}{AE}[\sigma(1) = \sigma(2)] \tag{1b}$$

$$\frac{t_d}{\Delta t_d} = \left(\frac{qV}{8kT}\right)^{1/2} \tag{1c}$$

where t_d is the drift time; σ the collision cross section; z the IC cell length; E the electric field across the cell; A a constant that depends on ion mass, charge (q), and the system's temperature (T); V the cell voltage; k the Boltzmann constant; and Δt_d the time width of an ion packet of a specific species attributable to collisional broadening in the cell. Equation 1b indicates that the time separation of two species in the ATD is directly proportional to the difference in their collision cross sections. Equation 1c gives the "resolution" of the device. To maximize resolution one needs to work at the highest allowable drift voltages and the lowest practical temperatures. In practice the buffer gas pressure limits the drift voltage since increasing the drift voltage also increases the translational temperature of the ions unless the pressure is increased commensurately. Since pumping capacity limits the pressure to ~5 Torr (at 300 K) in our machine, this limits the upper end of the voltage we can use. In a similar vein, lowering T increases resolution. As a practical matter our instrument is limited to 77 K. It turns out that this is not a restriction, however, since all mobilities go to the Langevin mobility as $T \rightarrow 0$. Hence, even though the peaks get narrower, they also get closer together. We have found that 150 ± 25 K provides maximum resolution in our experiment.

III. Met-cars and Other Metallo/Carbon Clusters

Certainly the event of the decade in cluster chemistry was the discovery[11] of the fullerene cage compounds, especially C_{60}. The ability to isolate them in bulk form[12] has ignited an incredible flurry of activity and created a large field of research that did not exist before 1990. It did not take long before researchers in this field realized that the carbon cage could encapsulate atoms, and endohedral metals were believed to have the most interesting properties.[24] In a parallel development, Castleman and co-workers[13]

(22) For all systems discussed in this paper this criterion holds.
(23) Kemper, P. R.; Bowers, M. T. *J. Phys. Chem.* **1991**, *95*, 5134.

(24) See, for example: Chui, Y.; Guo, T.; Jin, C. M.; Henfler, R. E.; Chubarte, L. P. F.; Fune, J.; Wang, L. H.; Alford, L. M.; Smalley, R. E. *J. Phys. Chem.* **1991**, *95*, 7564. Bethune, D. S.; Johnson, R. D.; Salem, J. R.; deVries, M. S.; Yannoni, C. S. *Nature* **1993**, *366*, 123. Pradeep, T.; Kulkarni, G.; Kannan, K.; Row, T. G.; Rao, C. J. *J. Am. Chem. Soc.* **1992**, *114*, 2272.

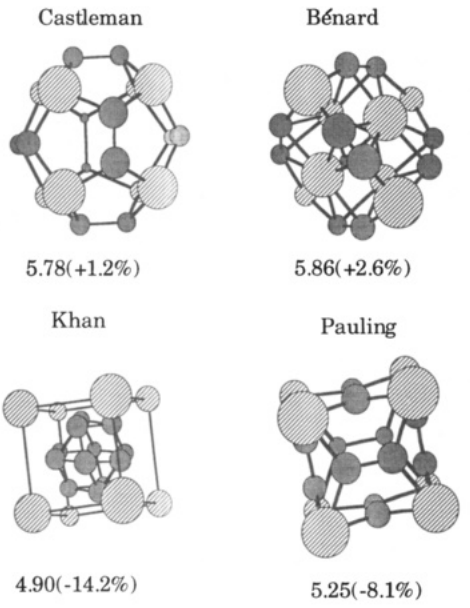

Figure 2. Several proposed Ti_8C_{12} met-car structures. Beneath each structure is the mobility (in $cm^2\ V^{-1}\ s^{-1}$) predicted using a Monte Carlo technique (ref 15b). Also shown is the percent deviation from the experimental mobility ($5.71 \pm 0.05\ cm^2\ V^{-1}\ s^{-1}$). The structures proposed by Castleman and Bénard fall within the acceptable range for a fit ($\sim\pm2\%$) while those proposed by Khan and Pauling do not. References for each structure are given in the text.

discovered another stable metal/carbon compound, the so-called metallocarbohedranes, or met-cars. These species have a stoichiometry of M_8C_{12}. A "magic" peak would often occur in the mass spectrum for ions of this mass. Castleman proposed a pentagonal icosahedral hollow cage structure for the met-cars.[13] Subsequently theoretical work[25] has suggested that related cage structures may be somewhat more stable for M = Ti. Two additional structures for the met-cars have also been proposed: a cubic structure by Pauling[26] with the Ti atoms occupying the corners of the cube and a pair of C atoms centered on each face, and a novel structure by Khan[27] where the Ti atoms again form a cube and the 12 C atoms from a ball inside it. These structures are given in Figure 2.

We have recently completed experimental work on the $Ti_8C_{12}^+$ system as well as the closely related $Ti_7C_{12}^+$, $Ti_8C_{11}^+$, $Ti_7C_{13}^+$, and $Ti_8C_{13}^+$ clusters. These ions were made using the LV−SSE source with CH_4 seeded in the He expansion gas. The details are given elsewhere.[28] The cluster of interest is mass selected and injected into the chromatography cell. In all cases the IC spectrum consisted of a single peak (see next section for examples of multiple peaks in an IC spectrum). From the arrival time at the detector it is possible to accurately extract the mobility, K, of the cluster as it passes through the He buffer gas ($K = v_d/E$). Using the structures given in Figure 2, mobilities can be calculated for each isomer using a Monte Carlo simulation technqiue.[15b] The results are shown below each structure along with the percent deviation from the experimental value. From many such comparisons in carbon clusters we deduce that an agreement between experiment and a modeled mobility had to be at least $\pm2\%$ for a positive identification to be made. Since these clusters contain both Ti and C atoms, and since the van der Waals radius of Ti is not precisely known,[29] a slightly larger deviation may occur in the met-car systems even for a correct structural assignment. Clearly the "cubic" structures of Khan and Pauling are not observed experimentally. The pentagonal icosahedron proposed by Castleman gives very good agreement with experiment as does the similar structure proposed by Bénard and coworkers.[30] The IC method cannot distinguish between the relatively small differences in these structures. What is absolutely clear is that a cage structure similar to the one first proposed by Castleman is in fact the met-car structure.

Pilgrim and Duncan[14] have made a series of interesting observations on Ti/C clusters. They observed a series of "magic" peaks in their mass spectra at masses above the mass of Ti_8C_{12}. They assigned these as members of a "cubic" family of structures, Ti_nC_m, where $m \cong n$. The most prominent of these is $Ti_{14}C_{13}^+$, a species predicted to be particularly stable by theory.[31] They then carried out the interesting photodissociation experiment

$$Ti_{14}C_{13}^+ \xrightarrow{nh\nu} Ti_8C_{13}^+ + 6Ti \qquad (2)$$

where loss of six Ti atoms is the dominant process. If $Ti_{14}C_{13}^+$ is cubic, then loss of the six face-centered Ti atoms would form a cube similar to Pauling's structure in Figure 2, except that the C atoms would be centered on the cube edges, and the thirteenth C atom would be endohedral. It would then be a relatively straightforward isomerization to form an endohedral met-car with a structure similar to either Castleman's or Bénard's in Figure 2. We have also observed $Ti_8C_{13}^+$ coming directly from our LV−SSE source. The IC signal consists of a single peak. We have modeled the endohedral structures described above and an exohedral structure where the "thirteenth" carbon atom is attached to a single Ti atom. Comparison of the model mobilities[15b] of these structures with experiment is given in Table 1. Clearly the exohedrally bound C atom best fits our data. This is not at all surprising since we are "growing" our clusters in the plasma expansion, and it appears that a C atom simply attaches itself to the cube face as a first step for further growth beyond the met-car. The $Ti_8C_{13}^+$ structure formed by photon-induced loss of six Ti atoms from $Ti_{14}C_{13}^+$ might well have a different structure, and the endohedral met-car is certainly a likely candidate. This is a perfect example that what you get "going up" may be very different from what you get "coming down" since both our experiment and that of Pilgrim and Duncan are kinetically rather than thermodynamically controlled. It would, of course, be very interesting to structurally interrogate the $Ti_8C_{13}^+$ cluster formed from photodissociation of $Ti_{14}C_{13}^+$, but this difficult experiment will have to wait.

(25) Dance, I. G. *J. Chem. Soc., Chem. Commun.* **1992**, 1779. Rohmer, M.-M.; Bénard, M.; Henriet, C.; Bo, C.; Poblet, J.-M. *Ibid.* **1993**, 1182. Lin, Z.; Hall, M. B. *J. Am. Chem. Soc.* **1993**, *115*, 11165.
(26) Pauling, L. *Proc. Natl. Acad. Sci. U.S.A.* **1992**, *89*, 8125.
(27) Khan, A. *J. Phys. Chem.* **1993**, *97*, 10937.
(28) Lee, S.-H.; Gotts, N.; von Helden, G.; Bowers, M. T. To be published.
(29) We actually determine initial estimates of van der Waals radii by calculating potential energy surfaces between the species of interest and a He atom.
(30) Rhonert, M.; de Vaal, P.; Bénard, M. *J. Am. Chem. Soc.* **1992**, *114*, 9696.
(31) Reddy, B. V.; Khanna, S. N. *Chem. Phys. Lett.* **1993**, *97*, 4616.

Table 1. Comparison of Model Mobilities with Experimental for $Ti_8C_{13}^+$

structure	mobility $cm^2/(V\cdot s)$	% deviation
endohedral cubic[a]	4.67	−14.9
endohedral met−car 1[b]	5.78	5.3
endohedral met−car 2[c]	5.90	7.5
exohedral met−car 1[d]	5.59	1.8
experiment	5.49	

[a] The mobility in the model assumed that the location of the remaining atoms in the $Ti_{14}C_{13}$ cube remained unchanged by the loss of the six face-centered Ti atoms. If the structure relaxes to a Pauling like structure (Figure 2), then the mobility becomes 5.25 and the deviation is −4.4%. [b] Using the Castleman structure, unchanged from Figure 2. If the presence of the endohedral C atom were to be included, calculations indicate that the structure would contract slightly (~1%), and the mobility would increase a commensurate amount. [c] Using a Bénard type structure reoptimized for the endohedral C atom. [d] The same Ti−C bond length was used for the exohedral C atom as the averate of the Ti−C distances in the cube. If this bond length were slightly longer, a perfect fit with experiment would be obtained. A Castleman type met−car was assumed for the cage.

If $Ti_8Cl_{12}^+$ is injected into the IC cell at high energy, collisional loss of Ti gives the only observed product. Since the collisional loss of Ti occurs very near the beginning of the cell, a chromatogram of the $Ti_7C_{12}^+$ product can be obtained.[28] Only a single peak is observed with a mobility of 6.00 $cm^2/(V\cdot s)$. If the met-car cage is kept completely rigid and a Ti atom removed, then a mobility of 5.91 $cm^2/(V\cdot s)$ is obtained. In reality, some relaxation will occur, which will slightly contract the cage, leading to a slightly larger model mobility.

If a carbon atom is removed, forming $Ti_8C_{11}^+$, a cluster we observe coming from the source but cannot make by CID of $Ti_8C_{12}^+$, a single IC peak of mobility 5.83 $cm^2/(V\cdot s)$ is obtained. If the unpaired C atom is placed at the center point of the C−C bond that would exist in $Ti_8C_{12}^+$, then a model mobility of 5.8 $cm^2/(V\cdot s)$ is obtained. In both of these instances it is clear that the integrity of the met-car cage structure is retained and that good estimates of the resulting structures can be obtained without having to resort to very difficult ab initio calculations on highly unsymmetric species.

One of our goals is to understand the mechanism of formation of these interesting met-car species. Consequently we have begun to study the growth process of M_nC_x clusters for small values of n and x. Initially we started on $Ti_nC_x^+$ clusters, but we have temporarily abandoned this system since the nominal mass of Ti is 48 amu, or just 4 times the mass of the C atom. We have, however, successfully begun analyzing the growth process in $Fe_nC_x^-$ clusters. The iron system does form a stable met-car,[14b] and clues to the growth process should be available from analysis of the smaller clusters in this series. What is needed is a way to explain the exclusive appearance of the $-MC_2-$ unit in the met-car cage.

Our initial results[32] indicate that for FeC_x^-, with x = 3−8, a mixture of linear and monocyclic species is observed; the x = even species tend to be linear, and the x = odd species tend to be cyclic. For $Fe_2C_x^-$ clusters only planar monocyclic rings are observed with the two Fe atoms bonded to each other. In the $Fe_3C_x^-$ series again only a single family of structures is observed. This time, however, the structures are three-dimensional. Many structural types were modeled, and the one that best fit the data added the third Fe atom above the plane of the ring (of the $Fe_2C_x^-$ species). It was bonded to both Fe atoms in the ring and the C_2 moiety most distant from the two Fe atoms. This bonding puckered the ring, giving it a baseball glove shape. The carbon chain was still completely intact, but it appeared that incipient Fe−C_2 moieties might be emerging.

Theoretical work in our group was used to confirm stabilities of structural families. Of particular interest was the fact the Fe atoms tended to charge transfer to carbon, forming electrostatic Fe^+---C_x^- species. Hence, the driving force to form met-cars could be the tendency to form $M^+-C_2^-$ units as size increases with the electrostatic contributions to the bonding overcoming the energy difference between the IP of M (typically 7.0 ± 0.5 eV for first-row metals) and the EA of C_2 (3.2 eV). The tendency to charge transfer will be accentuated for early metals since their IPs are about 1 eV less than those of late metals. Both theory and experiment will have to be pushed into the difficult "intermediate" region between Fe_3C_x and the formation of met-cars to confirm this suggestion or to formulate a different mechanism.

IV. Carbon Clusters and PAH's

As mentioned earlier, the ability to synthesize and isolate bulk quantities of C_{60} and several other fullerenes has set off an explosion of research on these interesting molecules. In almost all other instances, however, bulk quantities of clusters cannot be isolated and their properties must be determined "on the fly" from the relatively small amounts of material that can be formed in the gas phase. This also means that the properties of cluster *ions* are very much easier to determine than those of the neutrals in most cases since the very powerful methods of mass spectrometry can be brought to bear on them. Consequently, while the structure of C_{60} has been confirmed using traditional spectroscopic methods, the structures of almost all C_{60} carbon cluster precursors, except for a few small species,[33] have been determined only by the IC method.[15,19] The structural evolution of the fullerenes from these precursors is a complete story in its own right, and our current views will be told elsewhere.[34] Here, I want to comment on the fact that no PAH type carbon clusters, containing combinations of fused five- and six-membered rings in curved arrays, have been observed at any cluster size. This was initially very surprising since it was felt that growth of these PAH type precursors would lead eventually to fullerene formation.[11] Further, theory[35-38] suggested that these

(32) von Helden, G.; Gotts, N.; Maitre, P.; Bowers, M. T. *Chem. Phys. Lett.*, in press.

(33) Structural information has been inferred from photoelectron spectroscopy for small clusters and some structural parameters determined for several small linear clusters. See, for example: Yang, S. H.; Pettiette, C. L.; Conceicao, J.; Chisnoreski, O.; Smalley, R. E. *Chem. Phys. Lett.* **1988**, *144*, 431. Armold, C. C.; Zhao, Y.; Kitsopoulos, T. N.; Nuemark, D. M. *J. Chem. Phys.* **1992**, *97*, 6121. Heath, J. R.; Saykally, R. J. *The Structures and Vibrational Dynamics of Small Carbon Clusters*. In *On Clusters and Clustering*; Reynolds, P. J., Ed.; Elsevier: Amsterdam, 1993.

(34) Bowers, M. T.; von Helden, G.; Roskamp, E. J.; Jarrold, M. F. *Acc. Chem. Res.* To be published.

(35) Brabec, C. J.; Anderson, E.; Davidson, B. N.; Kajihura, S. A.; Zhang, Q. M.; Bernholc, J.; Tomanek, D. *Phys. Rev. B, Rapid Commun.* **1992**, *46*, 7326.

(36) Jensen, F.; Toftlund, H. *Chem. Phys. Lett.* **1993**, *201*, 89.

(37) von Helden, G.; Hsu, M.-T.; Gotts, N.; Kemper, P. R.; Bowers, M. T. *Chem. Phys. Lett.* **1993**, *204*, 15.

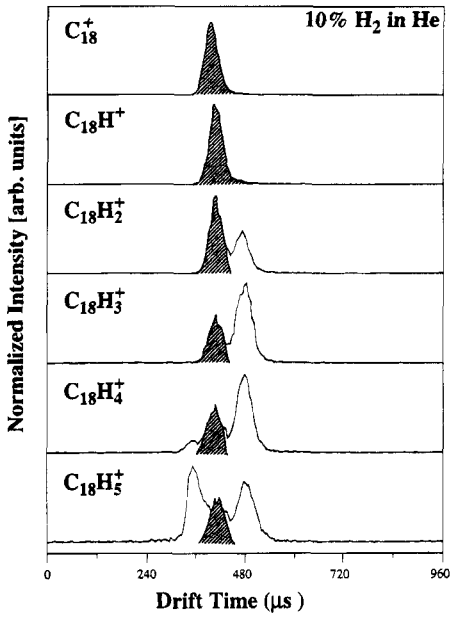

Figure 3. IC spectra for $C_{18}H_x^+$, $x = 0-5$. The cross-hatched peak corresponds to the monocyclic ring. The peak at longer times, beginning at $C_{18}H_2^+$, corresponds to a linear structure, and the one at shorter times, beginning at $C_{18}H_4^+$, to a bicyclic structure. The He pressure was 4.0 Torr, and the applied field, 12.5 V cm^{-1}.

bowl-shaped PAH type clusters should be stable for selected C_n clusters for $n \geq 20$.

One reason such structures might not appear in the LV–SSE experiments is that the kinetic pathways do not allow it. At small sizes carbon clusters are linear, and they begin to convert to monocyclic rings around C_7^+ for the cations[15,39] and C_{10}^- for the anions.[40] Monocyclic rings and larger bi- and tricyclic planar ring systems then dominate for both cations[15] and anions[41] for $n \leq 40$.

We have initiated two kinds of studies to try and find the missing PAH type carbon structures. In one effort we are starting with preformed PAH type structures that have the dangling bonds on the edges tied up with Cl atoms. The Cl_2 molecule makes an excellent leaving group, and we hope to follow the structure of these species as sequential Cl atoms depart. The second effort allows carbon cluster growth to occur in the usual way in a LV–SSE source, but some hydrogen is added to the He expansion gas. The idea is to see if the kinetics can be redirected if H atoms tie up a few of the dangling bonds.

When hydrogen is added to the He expansion gas, a number of interesting things happen.[42] First, the degree of clustering radically diminishes, with only a small fraction of the products with $n > 40$. Second, and most dramatic, the dominant structures change radically as hydrogen is added. For example, a set of chromatograms for $C_{18}H_x^+$, $x = 0-5$, is given in Figure 3. Previous studies[15] have shown that pure C_{18}^+ is

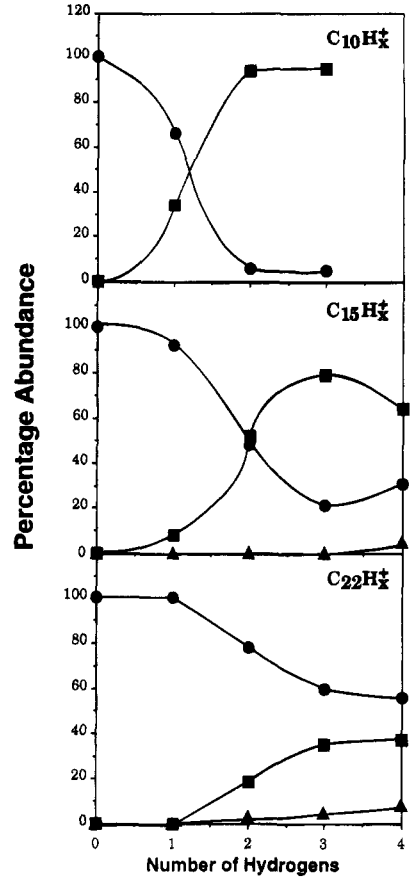

Figure 4. A plot of the percent isomeric composition in (a) $C_{10}H_x^+$, (b) $C_{15}H_x^+$, and (c) $C_{22}H_x^+$ for $x = 0-4$. The data were obtained from IC spectra such as those shown in Figure 3. The structures are linear (■), monocyclic (●), and bicyclic (▲). The lines connecting the points are only to guide the eye.

100% monocyclic ring. This monocyclic ring feature is shaded in the figure. Addition of one H atom does not change the structure, but for $x = 2$ a significant peak appears at longer times. This peak can be unambiguously assigned as a linear $C_{18}H_2^+$ structure. For $C_{18}H_3^+$ the linear structure dominates. At $x = 4$ an interesting thing happens. A significant feature at shorter times appears. We have assigned this fast moving peak as a bicyclic planar object,[42] and for $C_{18}H_5^+$ it becomes the largest peak in the IC spectrum. The area under each of these peaks can be determined, and the structural changes can be plotted as hydrogen is added. A sampling of these plots is given in Figure 4 for $C_{10}H_x^+$, $C_{15}H_x^+$, and $C_{22}H_x^+$ for $x = 0-4$. A number of interesting trends evolve. First, the effect of hydrogen on the structure is most evident for $C_{10}H_x^+$. For $x = 0$ C_{10}^+ is 100% cyclic; for $x = 1$ it is 65% cyclic and 35% linear; and for $x \geq 2$ it is essentially 100% linear. These are very dramatic changes, and while kinetics certainly enters into the formation of the structural distributions, thermochemistry must play a very large role as well. Clearly tying up the dangling bonds at the ends of the carbon chains greatly enhances their stability relative to cyclic species.

Of particular interest here is the onset of the first bicyclic cluster at $C_{15}H_4^+$. In pure carbon clusters[15] the first bicyclic cluster does not occur until C_{21}^+. It has been suggested that these bicyclic rings occur from the 2 + 2 "clipping together" of the two monocyclic

(38) Raghavachani, K.; Strout, D. L.; Odom, G. K.; Scuseria, G. E.; Opole, J. A.; Johnson, B. G.; Gill, P. M. W. *Chem. Phys. Lett.* **1993**, *314*, 357.
(39) von Helden, G.; Gotts, N.; Bowers, M. T. *Chem. Phys. Lett.* **1993**, *212*, 241. von Helden, G.; Palkee, W. E.; Bowers, M. T. *Ibid.* **1993**, *212*, 247.
(40) von Helden, G.; Kemper, P. R.; Gotts, N.; Bowers, M. T. *Science* **1993**, *259*, 1300.
(41) Gotts, N.; von Helden, G.; Bowers, M. T. To be published.
(42) Gotts, N.; Lee, S.-H.; von Helden, G.; Bowers, M. T. To be published.

Table 2. Structures of $C_{12}Cl_m^+$ Ions Derived from $C_{12}Cl_{10}$ (in Percent)[a]

structure	10	8	7	6	5	4	2	0
PAH	100*	100*	100*	89*	100*	69	0	0
bicyclic	0	0	0	0*	0*	0	0	0
monocyclic	0	0	0	11	0	23*	0	100*
linear	0	0	0	0	0	8	100*	0

[a] The number of Cl atoms retained is shown at the top of each column. The asterisk (*) denotes the most stable structure predicted by PM3 and AM1 calculations. Two asterisks in a column indicates essentially equivalent energies for the structures.

rings[15,43,44] although recent theoretical work suggests that a number of ring-clipping mechanisms may be competing.[45] In any case they are composed primarily of two large monocyclic rings probably coupled through a smaller four- or six-membered ring. The new bicyclic ring appearing in Figures 3 and 4 requires at least four hydrogen atoms and at least 15 carbon atoms. We have done extensive calculations using the semiempirical PM3 procedure[46] and have found that the lowest energy structure is a substituted benzene ring with two ortho hydrogens replaced by a pure C_9 carbon loop. The onset of the bicyclic structure at $C_{15}H_4^+$ is probably determined by ring strain in the loop. Interestingly, PM3 calculations indicate that the stability in pure carbon clusters has the order (from the most stable to the least stable) of C_n^+ (monocyclic ring) > C_n^+ (bicyclic) > C_n^+ (linear) while for $C_nH_4^+$ the order becomes $C_nH_4^+$ (bicyclic) > $C_nH_4^+$ (linear) > $C_nH_4^+$ (monocyclic) for $n \geq 15$. The great stability of the benzene ring drives the bicyclic species to lowest energy, and tying up all four dangling bonds on linear $C_nH_4^+$ fragments makes these structures more stable than the monocyclic rings. Addition of hydrogen to the monocyclic ring is relatively destabilizing as it disrupts the cumulenic or acetylenic electronic structures of these rings.

While the hydrogenation work gives some clues to the onset of stable PAH type structures, a better bet comes from perchlorinated PAH type structures as starting points. These species have been shown to readily shed all of the attached Cl atoms under high-energy electron ionization to yield the pure C_n^+ ions.[47] Our idea is to start with preformed C_nCl_m PAH type compounds and observe structural changes as Cl is lost. Our first results[48] on the $C_{12}Cl_{10}$ system are summarized in Table 2. Representatives of the various structures we observe are given in Figure 5. The parent $C_{12}Cl_{10}^+$ ion retains the PAH type structure as expected. This multiring structure persists experimentally down to $C_{12}Cl_4^+$. The experimental results through $C_{12}Cl_5^+$ are consistent with the relative stabilities predicted by PM3 and AM1 calculations. Our experinece is that the semiempirical theories do quite well for carbon-based molecules in this size range. It is perhaps surprising then that the original carbon framework persists for $C_{12}Cl_4^+$ since the mono-

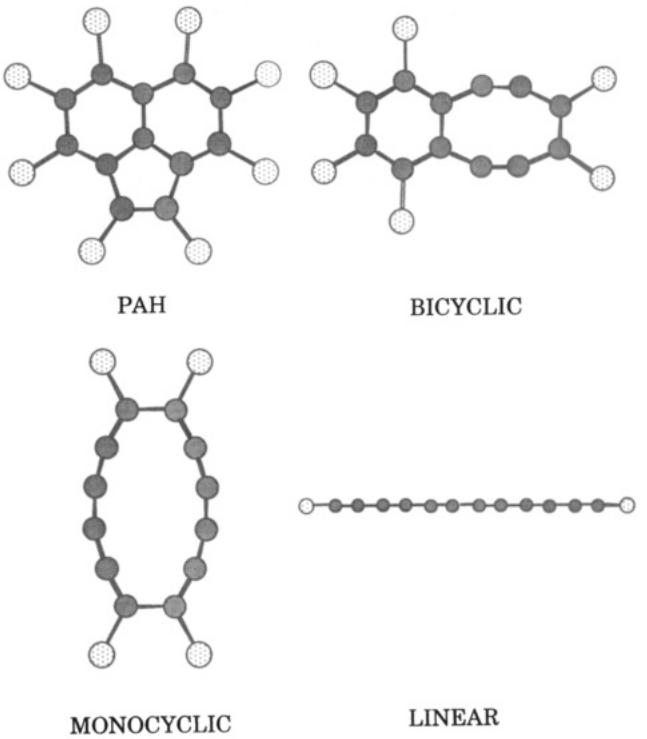

Figure 5. Typical structures of $C_{12}Cl_x^+$ clusters for various values of x (see Table 2).

cyclic ring is calculated to be 23 kcal/mol more stable. This suggests that there may be a barrier to rearrangement for $C_{12}Cl_4^+$, perhaps because the $C_{12}Cl_4^+$ bicyclic species is high in energy, and it may be an intermediate in the rearrangement reaction. It is not straightforward to rearrange from the PAH to the bicyclic structure due to the central carbon atom in the PAH type structure. Entropy should favor its formation, and hence it is surprising that it is the minor structural component. Again, a barrier to rearrangement may be involved. In fact, since these ions are formed by EI of $C_{12}Cl_{10}$, some of them may have very little internal energy and would thus retain the PAH type structure even if it is not the most stable form.

Once the $C_{12}Cl_4^+$ structure shown in Figure 5 is formed, loss of one Cl_2 molecule allows formation of the linear structure by simple cleavage of the remaining ClC−CCl bond. The $C_{12}Cl_2^+$ species is 100% linear, as predicted by theory, and loss of the final two Cl atoms induces ring closure to form 100% monocyclic C_{12}^+. This result is consistent with 100% monocyclic ring for C_{12}^+ formed from laser desorption of graphite.[15]

The preliminary data for $C_{14}Cl_{10}$ is much more fragmentary. However, it appears that C_{14}^+ formed from loss of all 10 Cl atoms has a pure monocyclic ring structure. Hence, larger PAH type frameworks will be required if pure carbon PAH type molecules are to be formed. Currently, work is underway[49] to study species as large as $C_{24}Cl_{14}$. We are encouraged by our initial work and have every expectation that we will eventually isolate a pure carbon cluster with a PAH type structure.

(43) von Helden, G.; Hsu, M.-T.; Kemper, P. R.; Bowers, M. T. Novel Forms of Carbon. *Mater. Res. Soc. Symp. Proc.* **1992**, *270*, 117.
(44) Hunter, J. M.; Fye, J. L.; Roskamp, E. J.; Jarrold, M. F. *J. Phys. Chem.* **1994**, *98*, 1810.
(45) G. Scuseria, private communication.
(46) Steward, J. J. P. *J. Comput. Chem.* **1989**, *10*, 209.
(47) Lifshitz, C.; Peres, T.; Kababiu, S.; Agranat, I. *Int. J. Mass Spectrom. Ion Processes* **1988**, *82*, 193. Lifshitz, C.; Sander, P.; Grutzmacher, H.-F.; Sun, J.; Weiske, T.; Schwarz, J. *J. Phys. Chem.* **1993**, *97*, 6592. Sun, J.; Grutzmacher, H.-F.; Lifshitz, C. *J. Am. Chem. Soc.* **1993**, *115*, 8382.
(48) von Helden, G.; Gotts, N.; Bowers, M. T. To be published.
(49) This work is a collaborative effort with Prof. Hans Grutzmacher at the University of Beilefeld in Germany.

Table 3. Experimental Binding Energies ($-\Delta H°_0$) in kcal/mol for[a]

$$M^+(H_2)_{n-1} + H_2 \rightleftharpoons M^+(H_2)_n$$

n	K^+ [i]	Sc^+ [f]	Ti^+ [g]	V^+ [j]	Fe^+ [e,g]	Co^+ [h]	Zr^+ [e,g]	Nb^+ [e,g]
1	1.45	5.5[b] (2.1)[c]	7.5	10.2	12.6	18.2	16.5[d]	14.8
2	1.35	6.9	10.0	10.7	16.7	17.0	11.8	15.6
3		5.4	9.3	8.8	8.5	9.6	11.5	14.3
4		5.0	9.4	9.0	9.8	9.6	11.0	15.4
5		4.5	9.7	4.2	2.7	4.3	10.6	16.6
6			9.5	9.6	2.6	4.0	10.3	14.3
7						0.8	9.9	13.4

[a] Where no data is recorded, the cluster was too weak to be observed, indicating a very small binding energy. The average uncertainty in the data in this table is ±0.3 kcal/mol. [b] For inserted H−Sc⁺−H. [c] For uninserted $Sc^+(H_2)$. [d] For inserted H−Zr⁺−H. [e] These values will drop by ~1 kcal/mol when $\Delta H°_0$ is determined. [f] Reference 54. [g] Unpublished results. [h] Reference 55. [i] Reference 56. [j] Reference 57.

V. Cluster-Assisted σ-Bond Activation

The activation of σ-bonds by transition metal centers is of central importance in organometallic chemistry and has assumed a position of prominence in such studies in gas phase ion chemistry.[50-53] The problems associated with these studies are many, however, because transition metal ions often have several low-lying excited states, during their reactions numerous surface crossings can occur, and the concept of spin can be ambiguous yet important in determining reactivity. As a consequence, often heroic efforts are required to obtain unambiguous results on reaction rates, branching ratios, and energetics. On the other hand, the existence of these low-lying excited states is the primary reason why transition metals make such good catalysts and show versatility in their reactivity. One avenue we as physical chemists have taken toward determining the factors that contribute to activation of σ-bonds is the accurate measurement of binding energies and entropies of M^+ ions to such simple molecules as H_2. The IC technique allows us to assure that we are dealing with ground state species, a necessary condition for unambiguous results. Our hope is to critically examine the factors assumed to be important in σ-bond activation and invite theorists to actively interact in interpreting the data and in the design of new experiments.

Our results to date for hydrogen binding to transition metal ions are summarized in Table 3. These values were obtained by measuring gas phase equilibrium constants over a wide temperature range. While details are found elsewhere,[54-57] a few points can be readily deduced from these data. (1) The solvation shell for the first-row metals is six, and this expands to eight for the second row, a result consistent with high-level electronic structure calculations we are pursuing in our lab. This point will be discussed further below regarding Sc^+, Zr^+, and Nb^+. (2) For Ti^+ and Fe^+ the first H_2 ligand is bound less strongly than the second. Both these ions have $3d^n4s^1$ ground states and low-lying $3d^{n+1}$ first excited states. We have shown numerous times that $3d^{n+1}$ configurations bind ligands much much strongly than $3d^n4s^1$ configurations because the 4s orbital is large in size and interacts repulsively with the ligand. Hence, in these two instances the $3d^n4s^1$ ground states of Ti^+ and Fe^+ cross over to the states that correlate to the $3d^{n+1}$ asymptotic M^+ excited state as the H_2 ligand approaches the metal center. The difference in binding energies between the first and second ligands is very nearly equal to the $3d^24s^1 \rightarrow 3d^3(Ti^+)$ and $3d^64s^{-1} \rightarrow 3d^7(Fe^+)$ promotion energies. (3) The sixth H_2 ligand is bound much more strongly than the fifth for V^+. This results from a high-spin−low-spin transition on the V^+ core on adding the sixth H_2 molecule [i.e., V^+ (a ^5D) → V^+ (a ^3P) in terms of asymptotic states]. While the spin change "costs" 32 kcal/mol, this energy is more than compensated for by the increase in bonding of all six ligands to V^+ in the ^3P state. In the quintet state there is essentially no charge transfer occurring between the ligands and V^+ since the d−d exchange energy on V^+ is so strong. In the triplet state there is substantial back donation into the σ* orbitals of four of the H_2 ligands from the filled π orbital on V^+ as well as H−H σ−bond donation into the empty σ orbital on V^+. Both of these interactions are promoted by increasing the d−d exchange on V^+. To this square planar $V^+(H_2)_4$ core the two final H_2 ligands add above and below the plane to complete an octahedral overall structure. This structure is estimated to be ~36 kcal/mol more stable for the V^+ ^3P core state than the ^5D core state, more than overcoming the 32 kcal/mol promotion energy.[57]

The following effect is not evident in the data of Table 3 but is very important. In virtually all measurements equilibrium was obtained on a time scale too short to measure under our experimental conditions. There are three exceptions: the addition of the first H_2 ligand to Sc^+ and Zr^+ and the addition of the seventh H_2 ligand to Nb^+. In each instance it took a very long time for equilibrium to become established. Clearly there should be no barrier involved in the simple formation of an M^+-H_2 bond, and consequently something else must be going on. For Sc^+ and Zr^+ it appears that insertion of the metal into the H−H bond occurs. This may also occur for $Nb^+(H_2)_6$, but this point is still being investigated. The Sc^+ system has been analyzed in great detail[54] and will be briefly presented here.

The interaction of Sc^+ in its (3d4s ^3D) ground state and (3d4s ^1D) and ($3d^2$ ^1D) excited states has been theoretically investigated in detail.[58,59] The results of these calculations as well as those done in our laboratory lead us to formulate the reaction coordinate diagram in Figure 6.[54] A number of points should be made at this juncture. First, insertion of ground state

(50) Eller, K.; Schwarz, H. *Chem. Rev.* **1991**, *91*, 1121.
(51) *Gas Phase Inorganic Chemistry*; Russel, D. H., Ed.; Plenum Press: New York, 1989.
(52) Weisshaar, J. C. *Adv. Chem. Phys.*; Ng, C., Ed.; Wiley-Interscience: New York, 1992, Vol. 82; *Acc. Chem. Res.* **1993**, *26*, 213.
(53) Armentrout, P. B. *Annu. Rev. Phys. Chem.* **1990**, *41*, 313; *Science* **1991**, *251*, 175.
(54) Bushnell, J. E.; Kemper, P. R.; Maitre, P.; Bowers, M. T. *J. Am. Chem. Soc.*, in press.
(55) Kemper, P. R.; Bushnell, J.; von Helden, G.; Bowers, M. T. *J. Phys. Chem.* **1993**, *97*, 52.
(56) Bushnell, J. E.; Kemper, P. R.; Bowers, M. T. *J. Phys. Chem.* **1994**, *98*, 2044.
(57) Bushnell, J. E.; Kemper, P. R.; Bowers, M. T. *J. Phys. Chem.* **1993**, *97*, 11628.
(58) Irikura, K. K.; Beauchamp, J. L. *J. Am. Chem. Soc.* **1989**, *111*, 75; **1991**, *113*, 2769; *J. Phys. Chem.* **1991**, *95*, 8344.
(59) Buckner, S. W.; Freiser, B. S. *J. Am. Chem. Soc.* **1987**, *109*, 1247. Gord, J. R.; Freiser, B. S.; Buckner, S. W. *J. Chem. Phys.* **1989**, *91*, 2530. Ranasinghe, Y. A.; MacMahon, T. J.; Freiser, B. S. *J. Phys. Chem.* **1991**, *95*, 7721.

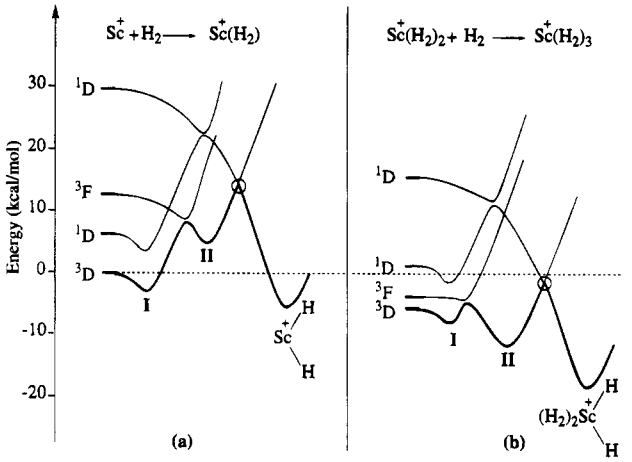

Figure 6. Slices through the potential energy surfaces for (a) the reaction of Sc^+ with H_2 and (b) the reaction of $Sc^+(H_2)_2$ with H_2. The asymptotic energies and the stationary points corresponding to structures **I**, **II**, H−Sc⁺H, and H−Sc⁺H$(H_2)_2$ are quantitative, and the remainders of the surfaces are approximate. The asymptotes in panel b correspond to the energies of $Sc^+(H_2)_2$ for SC^+ ions originally in the electronic states noted. The dashed line is the zero of energy for ground state Sc^+ and nH_2 molecules. There are two avoided crossings in each panel (for example, between the ^3D and ^3F curves in panel a) and one spin−orbit-coupled crossing denoted by the open circle (○). This spin−orbit crossing is the insertion transition state. See text for fuller discussion.

$Sc^+(^3D)$ into H_2 is slightly exoergic. Second, a series of significant barriers are encountered that prevent insertion at near thermal energies. Third, the adiabatic path from ground state reactants to inserted products requires two surface crossings before insertion can occur. (Note that, for simplicity, we will refer to surfaces in terms of their asymptotic Sc^+ electronic states.) The first requires a 3d4s $^3D \rightarrow 3d^2\ ^3F$ transition. The initial importance of the transition is that it allows closer approach of Sc^+ to H_2 by removing the repulsive 4s electron. The second transition state, which is rate determining, allows access to the $3d^2\ ^1D$ surface which adiabatically correlates to inserted products. The net result is that Sc^+ only has access to the shallow (~2.0 kcal/mol) electrostatic well (depicted as **I** in Figure 6) at thermal energies and consequently initially forms Sc^+ (3d4s $^3D)(H_2)$. This species cannot be the $Sc^+(H)_2$ molecule experimentally detected, however, because it would form instantly (rather than after 10^6 or more collisions) and its binding energy must be much less than the 5.5 kcal/mol measured in the equilibrium experiment.

The key to understanding this system is to realize several points. First, $Sc^+(H_2)$ is not formed in isolation but rather in a high-pressure bath of pure H_2, and rapid subsequent clustering must occur. Second, the ^3F state is a $3d^2$ configuration, and comparison with other results (see Table 3) and high-level electronic structure calculations indicate that this state binds H_2 more strongly than the ^3D ground state (theory indicates by 6 kcal/mol per H_2 ligand). As a result, after the third H_2 ligand is added to Sc^+, the structure labeled **II** in Figure 6 becomes significantly more stable than structure **I**. This has the effect of dramatically shortening all Sc^+-H_2 distances (by 0.7 Å) *and* of pulling the rate-determining spin−orbit coupled transition state *below* the $Sc^+ + H_2$ energy asymptote. [Remember, the experiment is measuring the reaction $Sc^+ + H_2 \rightarrow Sc^+(H_2)$.] At this point insertion can occur

Scheme 1

$$Sc^+(4s3d^3D) + H_2 \rightleftharpoons Sc^+(^3D)H_2 \rightleftharpoons Sc^+(^3D)(H_2)_2 \rightleftharpoons Sc^+(^3D)(H_2)_3$$

$$Sc^+(^3D)(H_2)_3 \rightarrow Sc^+(d^2\ ^3F)(H_2)_3 \rightarrow H\!>\!H\ Sc^+(^1A_1)(H_2)_2$$

$$H\!>\!H\ Sc^+(H_2)_2 \rightleftharpoons H\!>\!H\ Sc^+(H_2) \rightleftharpoons H\text{-}Sc^+\text{-}H$$

thermally, and the H−Sc⁺H$(H_2)_2$ inserted species rapidly equilibrates with H−Sc⁺H(H_2) and H−Sc⁺H. This entire process is shown in Scheme 1.

Other evidence that a mechanism such as that given in Scheme 1 is operating can be found in a detailed consideration of the kinetics,[54] especially the observation that analysis of the approach to equilibrium for formation of $Sc^+(H)_2$ yields a rate constant of ~5 × $10^{-1}17$ cm^3/s (i.e., a reaction efficiency of ~10^{-7}) and this rate constant has a strong negative temperature dependence. This system is, to our knowledge, the first known example of cluster-mediated σ-bond activation by a transition metal center.

The above example is of substantial importance because it opens the door to a new class of reactions in an active research area. It also demonstrates the utility of building a base of understanding of the primary interactions of transition metal ions with simple molecules and the essential, symbiotic nature of the theoretical/experimental coupling on problems of this type. However, it is important to show that the cluster-assisted mechanism is a general process and can be applied to more practically oriented systems. Hence, we turned our attention to another simple ligand whose σ-bond activation has tremendous possible import: CH_4. No first-row singly charged transition metals are known to activate CH_4, although several third-row metals[58] and doubly charged second-row metals[59] do so. The reason that first-row metals do not activate CH_4 is that their dehydrogenation reactions are all endoergic. Reaction 3, for example, is endoergic by about 20 kcal/mol for ground state Ti^+.

$$Ti^+ + CH_4 \rightarrow Ti^+{=}CH_2 + H_2 \qquad (3)$$

However, when three CH_4 molecules are complexed to Ti^+, a large peak is observed for loss of H_2. Hence, differential solvation by CH_4 of the dehydrogenated species relative to the nondehydrogenated species must be sufficient to overcome the 20 kcal endoergicity of reaction 3. These points are being further investigated both experimentally and theoretically.[60] The important point is that σ-bond activation of CH_4 is occurring for a first-row transition metal center.

VI. Conclusions

In this Account we have described several examples of cluster ions where novel and important chemistry is occurring. We have noted that the chemistry of the most versatile element, carbon, is complex and surprising. Its early chemistry is not dominated by "graphitic" or PAH type structures even though it is evident that fullerenes eventually become dominant species. We have described several experimental strategies to determine the size regime where these

(60) van Koppen, P. A. M.; Kemper, P. R.; Bushnell, J.; Maitre, P.; Bowers, M. T. To be published.

five- and six-membered-ring networks become competitive with large monocyclic rings.

We have also given the first unambiguous structural evidence that met-cars are indeed hollow cage compounds as first suggested by Castleman. The growth pattern of the metallo/carbon composites that eventually form these intriguing and potentially important species is completely unknown. From our initial work in small $Fe_nC_x^-$ clusters we suggest that charge transfer between the metal center(s) and small carbon units will be the driving force for forming the $-MC_2-$ building blocks of the met-cars.

Finally, we have discussed the important field of σ-bond activation by transition metal centers. Our focus here has been on cluster-assisted σ-bond activation in systems where either large barriers prevent metal insertion in the presence of only a single ligand or the insertion/elimination steps are endoergic under these conditions. The cluster-assisted mechanism appears to be quite general and allows activation of even the most difficult σ-bonds: those in H_2 and CH_4.

Many people in my research group contributed to the work in this Account. I'm especially indebted to Drs. Paul Kemper, Petra van Koppen, Gert von Helden, Nigel Gotts, Seung-Hoon Lee, and Philippe Maitre and to Mr. John Bushnell. I am also very grateful for support from the Air Force Office of Scientific Research and the National Science Foundation.